Biological Psychiatry: GOS

Archival Report

The Road Not Taken: Disconnection of a Human-Unique Cortical Pathway Underlying Naturalistic Social Perception in Schizophrenia

Gaurav H. Patel, David C. Gruskin, Sophie C. Arkin, Emery C. Jamerson, Daniel R. Ruiz-Betancourt, Casimir C. Klim, Juan P. Sanchez-Peña, Laura P. Bartel, Jessica K. Lee, Jack Grinband, Antígona Martinez, Rebecca A. Berman, Kevin N. Ochsner, David A. Leopold, and Daniel C. Javitt

ABSTRACT

BACKGROUND: Efficient processing of complex and dynamic social scenes relies on intact connectivity of many underlying cortical areas and networks, but how connectivity anomalies affect the neural substrates of social perception remains unknown. Here we measured these relationships using functionally based localization of social perception areas, resting-state functional connectivity, and movie-watching data.

METHODS: In 42 participants with schizophrenia (SzPs) and 41 healthy control subjects, we measured the functional connectivity of areas localized by face-emotion processing, theory-of-mind (ToM), and attention tasks. We quantified the weighted shortest path length between visual and medial prefrontal ToM areas in both populations to assess the impact of these changes in functional connectivity on network structure. We then correlated connectivity along the shortest path in each group with movie-evoked activity in a key node of the ToM network (posterior temporoparietal junction [TPJp]).

RESULTS: SzPs had pronounced decreases in connectivity in TPJ/posterior superior temporal sulcus (TPJ-pSTS) areas involved in face-emotion processing (t_{81} = 4.4, p = .00002). In healthy control subjects, the shortest path connecting visual and medial prefrontal ToM areas passed through TPJ-pSTS, whereas in SzPs, the shortest path passed through the prefrontal cortex. While movie-evoked TPJp activity correlated with connectivity along the TPJ-pSTS pathway in both groups (r = 0.43, p = .002), it additionally correlated with connectivity along the prefrontal cortex pathway only in SzPs (r_{SzP} = 0.56, p = .003).

CONCLUSIONS: These results suggest that connectivity along the human-unique TPJ-pSTS pathway affects both the network architecture and functioning of areas involved in processing complex dynamic social scenes. These results demonstrate how focal connectivity anomalies can have widespread impacts across the cortex.

https://doi.org/10.1016/j.bpsgos.2022.03.008

The ability to deftly navigate complex social situations is a key aspect of everyday human life (1). During real-life social perception, novel sensory information (e.g., detection of a changing facial expression) is used to update internal models critical to ongoing cognitive operations (e.g., theory-of-mind [ToM]/mentalization) to optimally guide behavior (e.g., who to look at next) (2,3). For the perception of these social cues to happen quickly, information must travel efficiently within and between the various cortical areas and networks underlying these processes [Figure 5 in (4)].

Task-based functional magnetic resonance imaging (fMRI) studies have individually found differences within each of the systems underlying visual social perception (face-emotion processing, ToM, and attention). However, in reality these systems are components of a larger network that transforms sensory information into behaviors such as eye movements based on cognitive operations. How these components interact and how functional differences in these components in participants with schizophrenia (SzPs) relate to each other remains unclear (5,6). Resting-state functional connectivity is often used to assess the degree of functional interaction because it partly reflects how efficiently or frequently any two areas communicate with each other during everyday cognitive processes (7). These relationships can be used to build a connectome that maps the cortical network structure. The shortest path between any two areas in this connectome, weighted by the strength of the connections along the path, is summarized as the weighted shortest path length (wSPL) (8). Thus, decreased connectivity between any path element (or edge) would result in increased wSPL, implying that the efficiency and/or communication between those two areas has decreased.

SEE COMMENTARY ON PAGE 314

ISSN: 2667-1743

A critical step in such analyses is the definition of cortical areas as nodes. However, the usual approach of using resting-state functional connectivity patterns to define and assign functions to cortical areas and networks has limitations. These include 1) the reverse inference problem, where the functional interpretation of differences in connectivity is often derived from these connectivity-based network labels, rather than the actual function governed by the areas; 2) a lack of agreement between parcellation schemes, especially in associative regions of the cortex; and 3) in the absence of labels pertaining to specific functions, such as face-emotion recognition, leaving no a priori method for identifying and studying these specific areas. Here, instead, we use a number of tasks designed to localize the brain areas underlying these key aspects of social perception to provide a more precise functional context within which connectivity anomalies can be interpreted.

We previously used these methods to detail the organization of the temporoparietal junction/posterior superior temporal sulcus (TPJ-pSTS) (4), a region with little consensus about its functional subdivision. In our model, the TPJ-pSTS is the core hub of a human-unique pathway linking the visual cortex, prefrontal cognitive control, and ToM areas that complements the dorsal and ventral visual pathways (2,9). Key components of the TPJ-pSTS include 1) the pSTS, involved in processing moving facial expressions; 2) the posterior TPJ (TPJp), critical to the performance of ToM operations; 3) the anterior TPJ, a key node of the ventral attention network involved in reorientating attention to behaviorally relevant stimuli, and 4) the middle TPJ (TPJm), a potential hub linking the other TPJ-pSTS areas.

In that study, we used a naturalistic visual stimulus—a 15-minute clip from the movie "The Good, the Bad, and the Ugly" with the soundtrack removed—to show that in SzP, the TPJ-pSTS pathway appeared to be functionally disconnected: it did not appropriately respond to visual motion inputs, did not appropriately communicate with other visual processing and attention areas, and was not appropriately involved in a key output behavior, saccades. Fidelity of TPJ-pSTS activation was also correlated with performance on a naturalistic test of social cognition, The Awareness of Social Inference Test (TASIT) (10), which we previously linked to the ability to orientate attention/gaze to moving facial expressions in peripheral vision (11). In another study that focused on visual processing and attention areas, we found that the resting-state functional connectivity of the late visual cortex in SzPs was reduced and that increased functional connectivity of prefrontal cognitive control areas correlated with performance on the attention task (12). Together, these results suggested that the decreased fidelity of TPJ-pSTS activation may originate in visual processing anomalies, and that prefrontal-based component systems may be used to compensate for these anomalies.

Here, we combined these datasets to test this hypothesis. We first searched for anomalies in resting-state functional connectivity between social perception areas and component systems. We then examined how any anomalies might affect the wSPL between visual and ToM (VisToM) components, allowing us to make inferences about how these anomalies may impact the functioning of the network. Finally, we tested these inferences by examining relationships between resting-state functional connectivity and the fidelity of the movie-evoked activation of a key ToM area, the TPJp. Based on our previous observations, we hypothesized that 1) the integrity of the TPJ-pSTS pathway is critical for intact functioning of the TPJp, 2) that the functional disconnection observed previously is linked to connectivity anomalies along the TPJ-pSTS pathway, and 3) that any connectivity anomalies along the TPJ-pSTS pathway would result in increased reliance on alternate processing pathways.

METHODS AND MATERIALS

Participants

A total of 42 SzPs and 41 healthy control subjects (HCs) were recruited with informed consent in accordance with New York State Psychiatric Institute's Institutional Review Board. All participants completed the resting-state fMRI portion of the study. The resting-state data reported in (12) represent a subset of these participants. Of these resting-state participants, 27 SzPs and 21 HCs also completed the movie-watching fMRI session, same as those reported in Patel *et al.* (4). Inclusion/exclusion criteria are listed in the Supplement.

Resting-State and Movie-Watching MRI Sessions

Participants were placed comfortably inside the MRI scanner. For the resting-state fMRI scans, participants were instructed to fixate on a centrally placed cross while blood oxygen level–dependent data were collected. Multiple 5.5-minute runs of blood oxygen level–dependent data were collected (median [interquartile range]: HC: 4 [3.75–5]; SzP: 4 [3–5]; t_{81} = 0.9, p = .4) using a multiband fMRI sequence (2-mm isotropic, repetition time = 850 ms, multiband factor = 6). Structural T1 and T2 (0.8-mm isotropic), along with distortion correction scans (B0 fieldmaps), were also acquired as required for use of the Human Connectome Project processing pipelines. Participants willing to return for a second MRI session viewed a video clip of the first 15 minutes of the cinematic movie "The Good, the Bad, and the Ugly" (United Artists, 1966) (13) with the sound removed while blood oxygen level–dependent data were collected during one continuous 15-minute acquisition (1049 MR frames) with the same parameters as the resting-state fMRI scans.

Image Processing

MRI data were preprocessed with the Human Connectome Project pipelines version 3.4 (14), which place the data into gray-ordinates in a standardized surface atlas (as opposed to voxels in a volume atlas). The functional data were additionally cleaned of artifact largely following the recommendations from Power *et al.* (15). An adaptive threshold was used to censor movement-related frames to minimize the effects of respiratory motion (16). The percentage of frames censored differed between groups by a small but significant amount (mean [SD]: HC: 14.6% [5.4%] vs. SzP: 20.1% [8.1%]; t_{81} = 3.6, p = .0006).

Localizing Social Perception Regions of Interest

Social perception areas were defined as regions of interest (ROIs) derived from three localizer tasks: 1) a task that contrasted activity evoked by moving versus static facial

expressions, designed to localize areas involved in face-emotion recognition (17); 2) a visual search task designed to activate areas involved in visual processing, visual attention, and cognitive control (12,18,19); and 3) a task designed to activate areas involved in ToM operations evoked during the viewing of a short animated video (20). Based on the localizers and prior studies, the resulting 98 areas were then subdivided into 28 component systems. Details about these tasks, how they were used to define the ROIs, and how they were divided into component systems are in the Supplement and have been described previously (4) for the localization of TPJ-pSTS ROIs.

Contrasting Resting-State Functional Connectivity Between SzPs and HCs

Pairwise resting-state functional connectivity was calculated by correlating the cleaned time-course of each ROI pair (Pearson correlations) within each participant. Between- and within-component connectivity was calculated by averaging ROI-ROI connectivity pairs within each component-component interaction. Matrices for each individual were then Fisher-z transformed and used to calculate both within-group averages and between-group contrasts using two-tailed *t* tests (Bonferroni-corrected for multiple comparisons). Custom scripts implemented in MATLAB 2019a (The MathWorks, Inc.) were used for this and all subsequent analyses. All reported correlations were covaried for group and the group × independent variable interactions.

Pathway Definitions and Analyses

To examine differences in VisToM pathways between groups, we thresholded the group-average component connectivity matrices (correlations strengths falling above a given percentile threshold) to then calculate the wSPL between left (L) early visual (EVis) and right (R) anteromedial ToM (amToM) components in the medial prefrontal cortex (PFC) [the site of the highest-level ToM operations (3)] after inversion of the connectivity weights to represent internodal distance (Brain Connectivity Toolbox; https://sites.google.com/site/bctnet/), repeated for every fifth percentile threshold between the 55th and 85th percentile. At all thresholds, this revealed the same two potential pathways, one running through the TPJ-pSTS and the other through the PFC. We then tested whether the pathways differed between individuals in each group by repeating the above wSPL calculation for each individual, counting whether each individual's VisToM path passed through a TPJ-pSTS pathway gate node (defined as whether the path included L or R pSTS) and/or a PFC pathway gate node (whether the path included L or R PFC or cingulo-opercular/salience nodes), summing these across individuals in each group and comparing the differences against a permuted null distribution, repeated for each percentile threshold between the 50th percentile and the 85th percentile. See Supplemental Methods for further details.

Relationship of TPJ-pSTS and PFC Connectivity With VisToM wSPL

To examine the relationship of specific component-component connectivity strengths and wSPL, we first correlated (Fisher-z transformed Pearson's correlation) the connectivity strength of each path element and the wSPL between each VisToM component. We then counted the number of negative correlations with $p < .05$ (stronger connectivity ↔ shorter wSPL) between the six visual/face processing (FaceProc) components and the ten ToM components (60 total correlations). Significance was assessed by comparing this count of negative correlations against a null distribution created by shuffling group label of both the individual connectivity values and wSPL matrices along with ROI label (multiple comparisons corrected for the number of path elements) and repeating the count. Reported *p* values are corrected for multiple comparisons. For the displayed L EVis to R amToM paths, we covaried for group and the group × connectivity interaction to determine whether the correlation was similar or different in the two groups. This was then repeated for the connectivity between L and R pSTS and FaceProc components.

Correlation of Connectivity to TPJp Movie-Evoked Activity

For the subset of individuals who performed the movie-watching experiment, we first calculated the amount of movie-evoked activity in the TPJp using intersubject correlation (ISC) (13). TPJp ISC values were calculated for each participant as the pairwise correlation of the TPJp ROI time-course for each individual and the TPJp time-courses of each HC participant. HC ISC values were calculated against the group of all other HCs. We then correlated component-component connectivity strengths with TPJp ISC values. Connectivity-ISC correlation values with a significance of $p < .05$ were entered into stepwise linear regression model that preserved terms that significantly increased the model F-statistic. Partial *r* values listed in Results are derived from the final regression model.

RESULTS

Demographics

Demographically, SzPs were matched to HCs, with a small increase in mean (SD) age (39.8 [10.8] vs. 34.9 [9.6], $p = .03$) in SzPs (Table 1). As shown previously in a subsample of these participants (11), SzPs were more impaired in TASIT Sarcasm versus TASIT Lie performance and on the Processing Speed Index. Other demographics and SzP characteristics are in Table 1. For the subset of participants who completed the movie-watching experiment, no significant demographic differences were found (4).

Parcellation of Brain Areas Activated by TASIT and the Movie-Watching Task

The functionally defined areas derived a priori from the localizer tasks (colored borders in Figure 1A and Figure S1) covered much of the cortex activated by both the TASIT social perception task (activation map in Figure 1A) and the activity (as measured by ISC) evoked by the visual-only movie-watching task (Figure 1B), with (as expected) the most significant discrepancy in the auditory cortex and superior temporal gyrus.

Table 1. Demographics, Scales, and Test Performance

Demographics/Performance	Healthy Control Subjects (n = 41)	Schizophrenia Participants (n = 42)	Statistics
Age, Years	34.9 (9.6)	39.8 (10.8)	$t_{80} = 2.2$, $p = .03$
Gender, Female/Male, n	18/23	10/32	$\chi^2_1 = 3.7$, $p = .05$
Race/Ethnicity, %			
Black	41.5%	45.2%	$\chi^2_1 = 0.12$, $p = .73$
Hispanic	12.2%	31.0%	$\chi^2_1 = 4.3$, $p = .04$
White	29.3%	30.9%	$\chi^2_1 = 0.03$, $p = .87$
Participant Education, Years	15.1 (1.9)	14.2 (2.7)	$t_{80} = 1.7$, $p = .09$
Participant SES	35.4 (13.4)	29.9 (13.1)	$t_{81} = -1.9$, $p = .06$
Edinburgh Handedness Score	15.2 (6.5)	17.1 (4.6)	$t_{76} = 1.6$, $p = .12$
IQ (WRAT Scaled Score)	100.4 (13.4)	96.3 (10.8)	$t_{65} = -1.4$, $p = .17$
TASIT A Sarcasm (Out of 32)	25.5 (4.3)	19.7 (5.0)	$t_{68} = 5.2$, $p < 1 \times 10^{-5}$
TASIT A Lies (Out of 32)	27.5 (3.2)	25.0 (4.4)	$t_{68} = 2.7$, $p = .009$
Processing Speed Index	104.5 (15.2)	88.4 (16.2)	$t_{77} = 4.5$, $p < 1 \times 10^{-4}$
MATRICS Composite T Score	–	43.0 (7.9)	–
PANSS Positive Symptoms	–	15.2 (5.6)	–
PANSS Negative Symptoms	–	13.5 (3.3)	–
PANSS Total Score	–	57.0 (13.6)	–
Antipsychotic Dose, CPZ Equivalents, mg, Mean (SD), n/n	–	434.3 (437.6), 37/42 on medication	–

Values are presented as mean (SD) unless otherwise indicated.

CPZ, chlorpromazine; PANSS, Positive and Negative Syndrome Scale; SES, socioeconomic stats; TASIT, The Awareness of Social Inference Test; WRAT, Wide Range Achievement Test.

Functional Connectivity of Social Perception Areas

Across all of the component systems, we observed significant reductions in SzPs in the within-system connectivity of the pSTS face-emotion recognition and lateral/ventral occipitotemporal FaceProc systems (Figure 2A; Figures S2 and S3). Focusing on these two components suggests that there may be a general reduction of the connectivity of the pSTS to other occipitotemporal components (Figure 2B; Figures S2 and S3). Figures S4 and S5 demonstrate the same general pattern of reductions in connectivity with the parcellation scheme from Glasser *et al.* (21). Covarying for the demographics that differed in Table 1 did not change these results (see Table S1).

Shortest Path Between VisToM Components

We next examined the effects of pSTS hypoconnectivity on network structure and efficiency. In Figure 3A, there appears to be two paths connecting visual areas to high-level ToM areas in the PFC. One path connects through the PFC and includes the dorsal attention and cingulo-opercular networks (PFC pathway, highlighted in orange). The other connects through areas in the pSTS and TPJ, including the TPJm hub area and the TPJp on the angular gyrus (TPJ-pSTS pathway, highlighted in green).

To examine how the pSTS hypoconnectivity in SzPs may affect the path of communication between visual and high-level ToM areas, we first compared the wSPL between the L EVis and R amToM component systems (Figure 3B). In HCs, the shortest path ran along the TPJ-pSTS path (green line), whereas in SzPs, the shortest path did not include any TPJ-pSTS components and instead ran along the PFC pathway components (orange dotted line). This group difference was similar across percentile thresholds (Figure 3C), with the shortest path crossing significantly more often through the TPJ-pSTS in HCs versus SzPs (Figure 3D, green bar). Within groups, the shortest path in HCs was most often along the TPJ-pSTS pathway (Figure 3D, blue bar) versus the PFC pathway in SzPs (Figure 3D, red bar). See the Supplement for discussion of characteristic path length.

Effects of pSTS and Face Processing Hypoconnectivity on VisToM wSPL

The results above suggested that reduced pSTS connectivity in SzPs may affect how the two paths—TPJ-pSTS and PFC—are used to efficiently connect VisToM components. We first examined whether pathway connectivity strength related to VisToM wSPL. For TPJ-pSTS path components (Figure 4A), the VisToM wSPL in both groups was strongly associated with L late visual (LVis)–R pSTS connectivity, with nearly all 60 component-component pairs demonstrating significant relationships in both groups (path element 2, Figure 4B). The slope of the relationship in SzPs was similar or stronger than HCs (Figure 4C; Figure S7). This relationship was similar for R LVis–R pSTS connectivity. R pSTS–R TPJm connectivity was also significantly correlated only in HCs (path element 3, raw $p = .0002$) but with similar slopes in both groups (connectivity: $F_{2,81} = 8.5$, $p = .005$). For the PFC pathway (Figure 4D), the connectivity of path elements 2 and 3 were associated with VisToM wSPL only in SzPs (raw $p < .00005$) (Figure 4E). Underlying these differences was a strong negative relationship in SzPs versus a minimal relationship in HCs (Figure 4F; Figure S8).

We then examined how pSTS and FaceProc connectivity related to VisToM wSPL. L to R pSTS connectivity (Figure 4G)

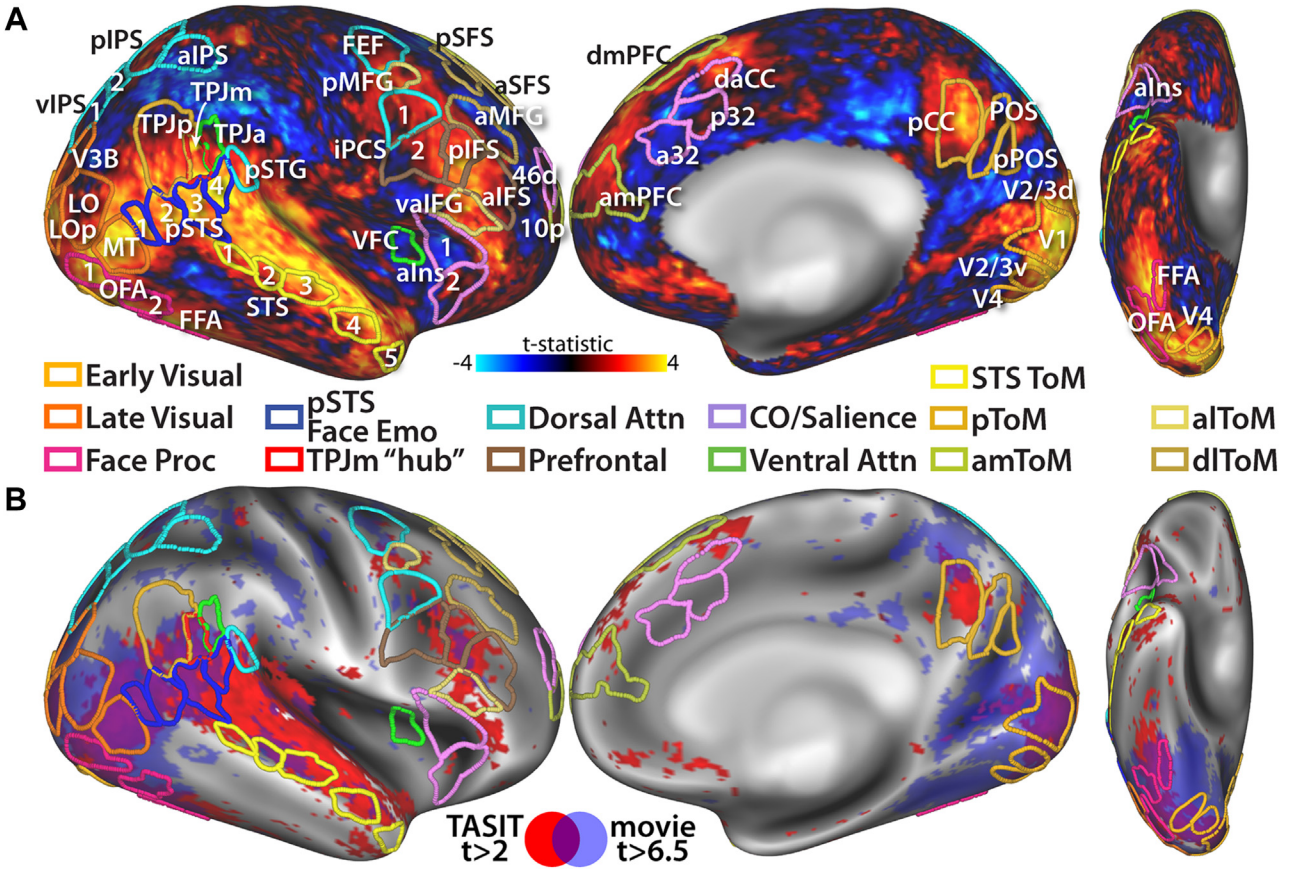

Figure 1. Cortical activation by naturalistic stimuli and region of interest definitions. **(A)** Activation evoked by The Awareness of Social Inference Test (TASIT) videos in 10 healthy control subjects are covered by regions of interest derived from functional localizers (with the notable exception of the auditory cortex). See Figure S1 for functional localizers and region of interest definitions. **(B)** Activation by TASIT (red) and activation by the cinematic movie "The Good, the Bad, and the Ugly" as measured by intersubject correlation (blue) largely overlap (purple). 10p, posterior area 10; 46d, dorsal area 46; a32, area 32; aIFS, anterior inferior frontal sulcus; aIns, anterior insula; aIPS, anterior intraparietal sulcus; alToM, anterolateral ToM; aMFG, anterior middle frontal gyrus; amPFC, anterior medial prefrontal cortex; amToM, anteromedial ToM; Attn, Attention; CO, cingulo-opercular; daCC, dorsal anterior cingulate cortex; dlToM, dorsolateral ToM; dmPFC, dorsal medial prefrontal cortex; Emo, emotion; FEF, frontal eye-field; FFA, fusiform face area; iPCS, inferior precentral sulcus; LO, lateral occipital; LOp, lateral occipital posterior; MT, medial temporal; OFA, occipital face area; p/aSFS, posterior/anterior superior frontal sulcus; pCC, posterior cingulate cortex; pIPS, posterior intraparietal sulcus; pMFG, posterior middle frontal gyrus; POS, parietal/occipital sulcus; pPOS, posterior parietal/occipital sulcus; Proc, processing; pSTG, posterior superior temporal gyrus; pSTS, posterior superior temporal sulcus; pToM, posterior ToM; STS, superior temporal sulcus; ToM, theory-of-mind; TPJa, anterior temporoparietal junction; TPJm, middle temporoparietal junction; TPJp, posterior temporoparietal junction; V.2/3v, ventral V.2 and V.3; vaIFG, ventral anterior inferior frontal gyrus; VFC, ventral frontal cortex; vIPS, ventral intraparietal sulcus.

correlated with VisToM wSPL in both groups with no significant group difference (raw $p_{HC} < .00005$, raw $p_{SzP} < .00005$) (Figure 4H, I). This was similar to the VisToM wSPL relationship with TPJ-pSTS path element 2 (Figure 4C); indeed, the L to R pSTS connectivity correlated strongly with the connectivity of TPJ-pSTS path element 2 in both groups, more in HCs than SzPs (group × pSTS connectivity: $F_{2,81} = 6.9$, $p = .01$; $r_{HC} = 0.69$, $p_{HC} < 1 \times 10^{-6}$; $r_{SzP} = 0.33$, $p_{SzP} = .035$).

However, L to R FaceProc connectivity only correlated with VisToM wSPL in SzP (raw $p_{HC} = .11$, raw $p_{SzP} = .005$, raw $p_{SzP\text{-}HC} = .002$) (Figure 4H) and also correlated strongly with connectivity of PFC pathway element 2 only in SzPs (group × FaceProc connectivity: $F_{2,81} = 7.3$, $p = .008$; $r_{HC} = 0.28$, $p_{HC} = .08$; $r_{SzP} = 0.68$, $p_{SzP} < 1 \times 10^{-6}$). FaceProc connectivity also correlated to a lesser extent with TPJ-pSTS path element 2 connectivity in both groups ($r_{HC} = 0.36$, $p_{HC} = .021$; $r_{SzP} = 0.34$, $p_{SzP} = .026$), and pSTS connectivity only correlated weakly with PFC path element 2 in HC ($r_{HC} = 0.33$, $p_{HC} = .038$; $r_{SzP} = 0.15$, $p_{SzP} = .35$).

Relation of Pathway Connectivity to the Functioning of ToM Areas During Naturalistic Stimulation

The above connectivity-wSPL analyses in Figures 3 and 4 suggest that reductions in pSTS connectivity in SzPs affect the use of the TPJ-pSTS pathway for VisToM communication, resulting in a shift to using a combination of the TPJ-pSTS and PFC pathways. In the subset of participants with movie-watching data, we tested this hypothesis by examining relationships between the connectivity of the path elements with the fidelity of the activation of the TPJp (Figure 5; Figures S9 and S10).

Entering all of these significant correlations from both pathways into a stepwise regression model, in HCs, three

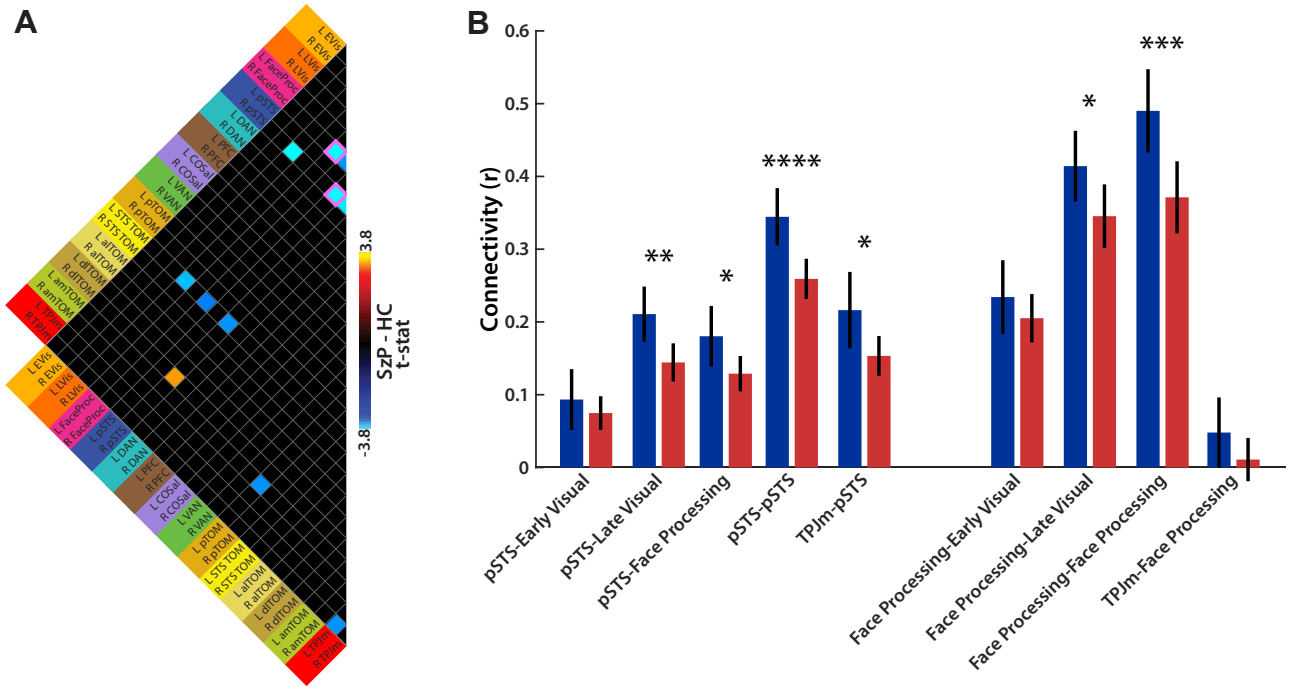

Figure 2. Contrast of component-to-component connectivity between participants with schizophrenia (SzPs) and healthy control subjects (HCs). **(A)** Differences between SzP and HC component connectivity are limited to the face processing and posterior superior temporal sulcus (pSTS) components. Matrix thresholded at $p < .01$. Purple outlines highlight differences that survive multiple comparisons at $p < .05$ (face processing: $t_{81} = 4.3$, Cohen's $d = 0.95$; pSTS: $t_{81} = 4.4$, Cohen's $d = 0.96$). **(B)** Detail of differences in SzP vs. HC connectivity of the face-processing and pSTS components with themselves, visual, and middle temporoparietal junction (TPJm) components. Raw (not corrected for multiple comparisons) p values shown. *$p < .05$, **$p < .01$, ***$p < .001$, ****$p < .0001$. alToM, anterolateral ToM; amToM, anteromedial ToM; COSal, cingulo-opercular salience; DAN, dorsal attention network; dlToM, dorsolateral ToM; EVis, early visual; FaceProc, face processing; L, left; LVis, late visual; PFC, prefrontal cortex; pTOM, posterior ToM; R, right; ToM, theory-of-mind; VAN, ventral attention network.

correlations survived, all specific to HCs and along the TPJ-pSTS pathway ($r^2 = 0.76$, $p = .00002$) (Figure 5A): R FaceProc to R posterior ToM (pToM) (partial $r = 0.53$, $p = .02$) (Figure 5B), R TPJm to R amToM (partial $r = -0.65$, $p = .003$) (Figure 5C), and R pSTS to L pToM (partial $r = -0.64$, $p = .003$). We also examined how the connectivity strength between path elements related to other path elements. Along the TPJ-pSTS pathway in HCs, the connectivity of R TPJm to amToM/pToM components was strongly negatively correlated with visual/FaceProc components to R TPJm connectivity (orange dotted line in Figure 5A) in both the movie subset ($r = -0.71$, $p = .0003$) and the complete resting-state dataset ($r = -0.70$, $p < 1 \times 10^{-6}$).

In SzPs, two correlations remained in the stepwise regression model ($r^2 = 0.44$, $p = .0009$) (Figure 5D): L to R PFC (partial $r = 0.56$, $p = .003$) (Figure 5E) in the PFC pathway and L pSTS to L pToM (partial $r = -0.44$, $p = .025$) (Figure 5F) in the TPJ-pSTS pathway, both specific to SzPs. Similar to HCs, along the TPJ-pSTS pathway L pSTS to L pToM connectivity was negatively correlated with L/R LVis to L pSTS connectivity ($r = -0.36$, $p = .02$ in the complete dataset and $r = -0.27$, $p = .18$ in the movie-watching subset).

DISCUSSION

In this study, we examined the functional connectivity of areas involved in the processing of naturalistic social scenes in SzPs versus HCs. First, we found focal reductions in connectivity in SzPs involving the pSTS face-emotion processing areas. Second, we found that the shortest path connecting visual areas to medial prefrontal ToM areas appeared to have shifted from the TPJ-pSTS pathway in HCs to the PFC pathway in SzPs. Third, we found that the VisToM wSPL was associated with the connectivity strength of TPJ-pSTS path elements in both groups and additionally with PFC path element connectivity strength only in SzPs. Fourth, we found that the pSTS connectivity appeared to have a stronger effect on VisToM wSPL compared with FaceProc connectivity. Together, these connectivity analyses suggested that a pSTS functional anomaly, reflected in decreased connectivity, may affect the use of the TPJ-pSTS pathway in SzPs, forcing increased reliance on the alternate PFC pathway. We then confirmed this hypothesis by finding that the fidelity of the movie-evoked activation of the TPJp, a key ToM area, was associated with the connectivity of TPJ-pSTS pathway elements in HCs but with both the TPJ-pSTS and PFC pathways in SzPs. Overall, these results demonstrate that not only can focal functional connectivity anomalies have widespread and distant functional impacts that are predictable from the network structure but also point to potential mechanisms of resilience in the face of these anomalies.

Comparison to Previous Studies

Previous functional connectivity studies of SzPs have not found the decreased connectivity profiles revealed here

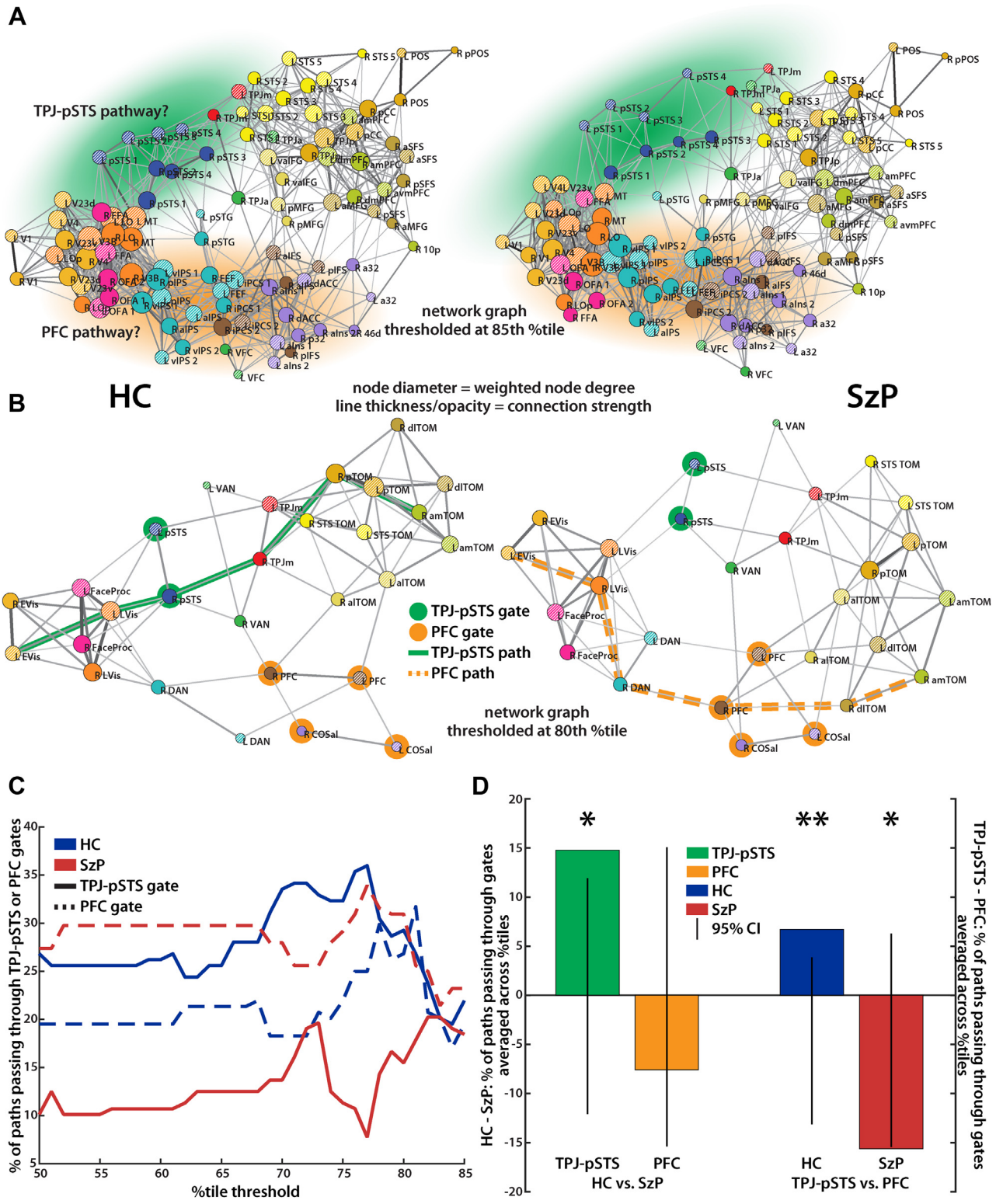

Figure 3. Group differences in the pathways connecting early visual (EVis) cortex and right medial prefrontal cortex (anteromedial theory-of-mind [amToM]). **(A)** Region of interest (ROI)–ROI network graphs for healthy control subjects (HC) and participants with schizophrenia (SzP). Spring-loaded graphs were produced in Pajek (http://mrvar.fdv.uni-lj.si/pajek/) and used to visualize the network architecture ROIs. The nodes in the graphs represent ROIs and are arranged such that the distance between any two nodes in the spring-loaded graph is inversely proportional to the similarity in their connectivity patterns with

(22–25), but our study is unique in two key ways. First, ours is one of the first to use high-resolution multiband sequences and surface mapping methods developed for the Human Connectome Project. This is of particular importance for the TPJ-pSTS, where high degrees of individual variability in sulcal geometry may obscure or blur potential differences in group averages and comparisons (26–28). Second, previously published parcellation schemes not only disagree greatly in the parcellation of the TPJ-pSTS, but also do not subdivide the TPJ-pSTS by function, with no designated face-emotion processing and attention reorientating areas (2). The resulting connectivity anomalies complement previous studies of visual processing and face-emotion recognition in schizophrenia. SzPs have long been noted to have a range of visual processing anomalies (29–33), including in face-emotion recognition (34,35) and the processing of biological motion (36). These anomalies have been linked to the lateral occipital cortex for visual processing (31,32) and the pSTS for face-emotion recognition (17). The functional connectivity reductions in this study likely reflect those functional anomalies and may represent disorganization or decreased/impaired use of this cortical region (37,38). Of note, the reduced connectivity in LVis areas described in (12) overlap with the reduced FaceProc connectivity but not the reduced pSTS connectivity observed here.

TPJ-pSTS as a Separate Processing Pathway

These results also support our model of the TPJ-pSTS representing a separate processing pathway linking visual and ToM areas, distinct from the classical dorsal/ventral visual processing pathways (both embedded in the PFC pathway) (2). As detailed in that review, this human-unique pathway allows for internal models of mental states to be more quickly updated by relevant incoming sensory information about social cues than the dorsal/ventral visual processing pathways embedded in the PFC pathway. This fast updating then leads to more efficient planning of eye movements and other relevant social behaviors. The connectivity-wSPL relationships in Figure 4 suggest that connectivity within the pSTS and with LVis is critical for this updating. While there may be other interpretations (i.e., a subcortical area driving both effects), we believe that our results suggest that pSTS hypoconnectivity has a lesion-like effect on the TPJ-pSTS pathway that then cripples its use in this updating. As a result, SzPs then appear to develop a unique reliance on the PFC pathway for this updating, as demonstrated by the SzP-specific correlations of FaceProc and PFC connectivity with the VisToM wSPL.

The movie-watching analyses suggest that efficient transmission of the visual information from visual/FaceProc components through the pSTS to the TPJ is critical for intact activation of the TPJp in HCs. However, in SzPs, intact TPJp activation is linked to both the TPJ-pSTS and PFC path components. These results also suggest that the reductions in TPJ activation fidelity observed previously by our group (4) were downstream of pSTS face-emotion processing anomalies as opposed to being rooted in the TPJ itself. The idea of there being multiple pathways for these operations has to be true of course: macaques are still able to visually scan social scenes and perform limited ToM operations despite having only the PFC pathway but not the TPJ-pSTS pathway (39).

Although unexpected, the strong negative correlations of TPJp ISC with the connectivity between high-level ToM components and both pSTS and TPJm suggest that decreasing the communication between these components may be just as important as increasing communication between visual and the TPJ-pSTS components. Although this may seem contradictory to the initial wSPL analyses presented in Figure 2, Figure 3 demonstrates that much of the path-shortening effect of the TPJ-pSTS pathway connectivity may be located in the path elements before TPJm.

PFC as a Compensatory Pathway

The fact that PFC pathway connectivity is associated with TPJp activation despite the TPJp not being a member of this pathway is particularly interesting and may complement a number of other observations we have made. First, in SzPs, we previously found that while the TPJ had decreased synchronization with visual areas, it had increased synchronization with prefrontal ToM and cognitive control areas (4). Second, we observed that in SzPs (but not HCs) only the Processing Speed Index from the Wechsler Adult Intelligence Scale-III IQ (WAIS-III) test was strongly associated with TASIT performance (11). The tasks that compose the Processing Speed Index all involve some degree of top-down driven visual search, which is guided by the dorsolateral PFC, the same areas that correlate with TPJp performance in this manuscript. These observations suggest that in SzPs, increased

other areas. The connectivity strength between nodes is represented by the thickness of the line connecting the nodes, and the number and strength of connections to that node (weighted node degree) is represented by the diameter of the nodes. Weighted node degree was chosen because it provides information about which components are most critical for the functioning of a network (40,41). ROI-ROI group-average connectivity matrices were thresholded at the 85th percentile before network graph visualization, and the Kamada-Kawai free-energy algorithm was used to arrange the ROIs. Component color codes are the same as Figure 1. Green shading highlights potential temporoparietal junction (TPJ)–posterior superior temporal sulcus (pSTS) pathway and orange shading the potential prefrontal cortex (PFC) pathway. **(B)** Component-component network graphs for HCs and SzPs in roughly the same spatial configuration as **(A)** but with nodes representing components instead of individual ROIs and group-average connectivity matrices thresholded at the 80th percentile. Green line highlights the shortest weighted path between left (L) EVis and right (R) amToM components in HCs. This path runs through the TPJ-pSTS gate (green highlighted nodes) and is hence labeled the TPJ-pSTS pathway. Orange dotted line highlights the shortest weighted path between L EVis and R amToM components in SzPs. This path runs through the PFC gate (orange highlighted nodes) and is hence labeled the PFC pathway. **(C)** The percentage of paths across individual participants in each group connecting L/R EVis and R amToM that run through the TPJ-pSTS gate nodes (highlighted in green) and/or the PFC gate nodes (highlighted in orange) as a function of the percentile threshold applied to create the graph. **(D)** The difference in the average percentage of paths passing through the gates for each of the four comparisons represented in **(C)** compared with a null distribution (represented by the line). Between groups, significantly more paths across HC participants run through the TPJ-pSTS than in SzPs (green bar) whereas the percentage of paths running through the PFC is similar in the two groups (orange bar). Within HCs, significantly more paths run through the TPJ-pSTS than the PFC (blue bar). Within SzPs, significantly more paths run through the PFC than TPJ-pSTS (red bar). $^{*}p < .05$, $^{**}p < .01$, both corrected for multiple comparisons. See Figure 1 legend for acronym definitions.

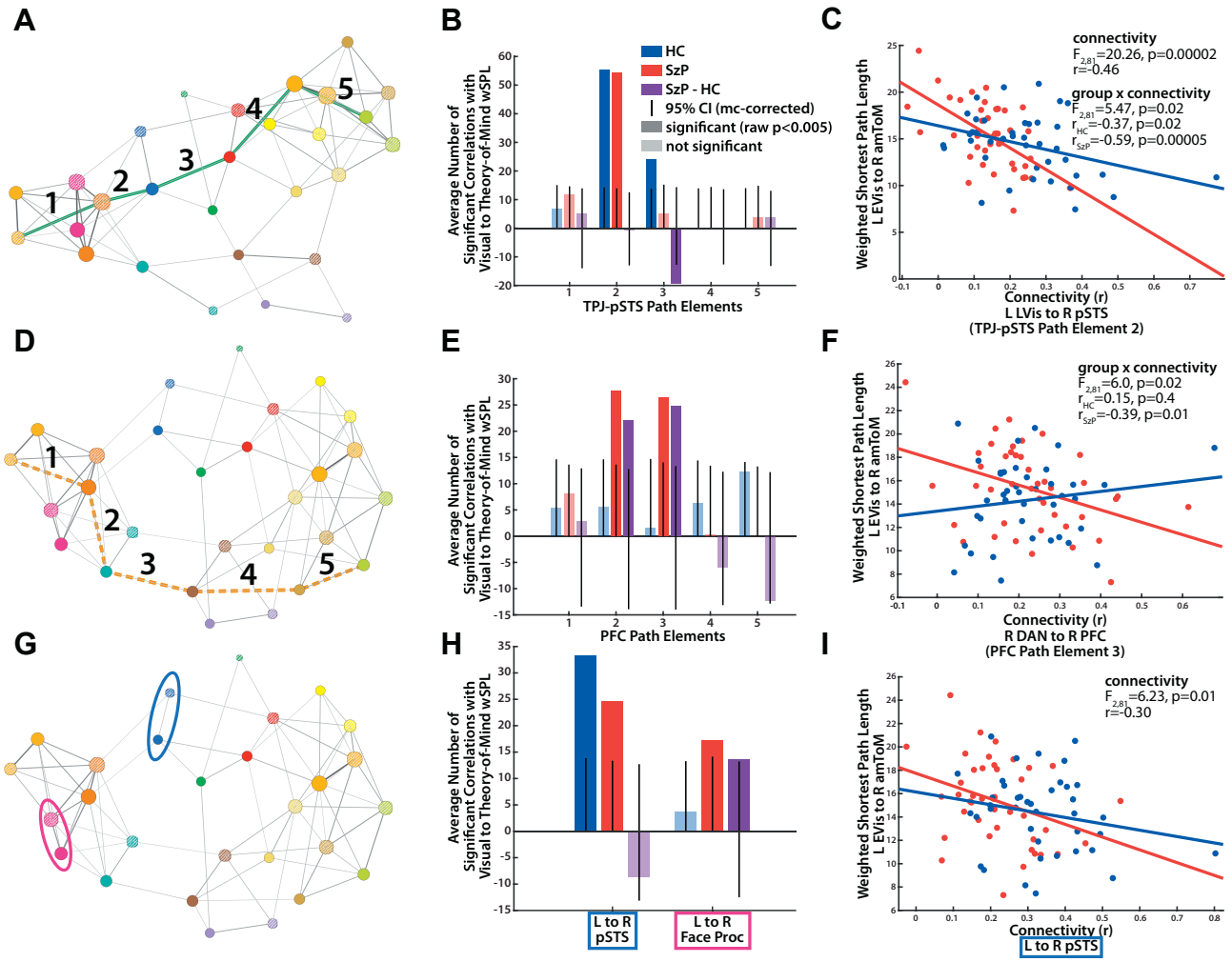

Figure 4. Relationship between connectivity strength between temporoparietal junction (TPJ)–posterior superior temporal sulcus (pSTS) and prefrontal cortex (PFC) path components and the weighted shortest path length (wSPL) between visual and theory-of-mind (VisToM) components. **(A)** The five path elements (or edges) of the TPJ-pSTS pathway. **(B)** The number of significant ($p < .05$) correlations between the connectivity of each TPJ-pSTS path element and VisToM wSPL. Lines represent the 99.5% CI drawn from a permuted distribution (group and component labels shuffled and correlations recalculated 10,000 times). Darker bars represent statistically significant results that survive correction for multiple comparisons (raw $p < .005$); lighter bars represent nonsignificant results. **(C)** Relationship between connectivity strength of TPJ-pSTS path element 2 (left [L] late visual [LVis] to right [R] pSTS components) and L early visual (EVis) to R anteromedial theory-of-mind (amToM) wSPL. Negative correlation indicates that stronger connectivity is associated with shorter wSPL. **(D)** The five path elements (or edges) of the PFC pathway. **(E)** The number of significant ($p < .05$) correlations between the connectivity of each PFC path element and VisToM wSPL. **(F)** Relationship between connectivity strength of PFC path element 3 (R dorsal attention network [DAN] to R PFC components) and L EVis to R amToM wSPL. **(G)** The pSTS and face processing (FaceProc) connections found to be significantly weaker in participants with schizophrenia (SzP) (Figure 2). **(H)** The number of significant ($p < .05$) correlations between the connectivity of L to R pSTS and L to R FaceProc components and VisToM wSPL. **(I)** Relationship between L to R pSTS connectivity strength and L EVis to R amToM wSPL. HC, healthy control subjects.

communication of visual information to the ToM network through the PFC may compensate for the damage to the TPJ-pSTS pathway and improve fidelity of TPJp activity. In addition, the visual strategy enacted by use of the PFC pathway could also result in differences in the relationship between visual scanning and ToM operations, as we observed recently (11).

Limitations and Future Directions

These results suggest causal relationships between pSTS hypoconnectivity, social perception network architecture, and ToM functioning, but causality will need to be directly tested with methods such as transcranial magnetic stimulation. Also, while these results demonstrate several previously unreported organizational principles and relationships and complement those reported in previous studies from our group (4,11), they come from overlapping samples and therefore the results will need to be replicated in an independent sample. In addition, in the movie-watching study, we found a relationship between TPJ activity and TASIT performance, but larger samples will allow for the study of the relationship between the integrity of these pathways, the functioning of the TPJ and other ToM

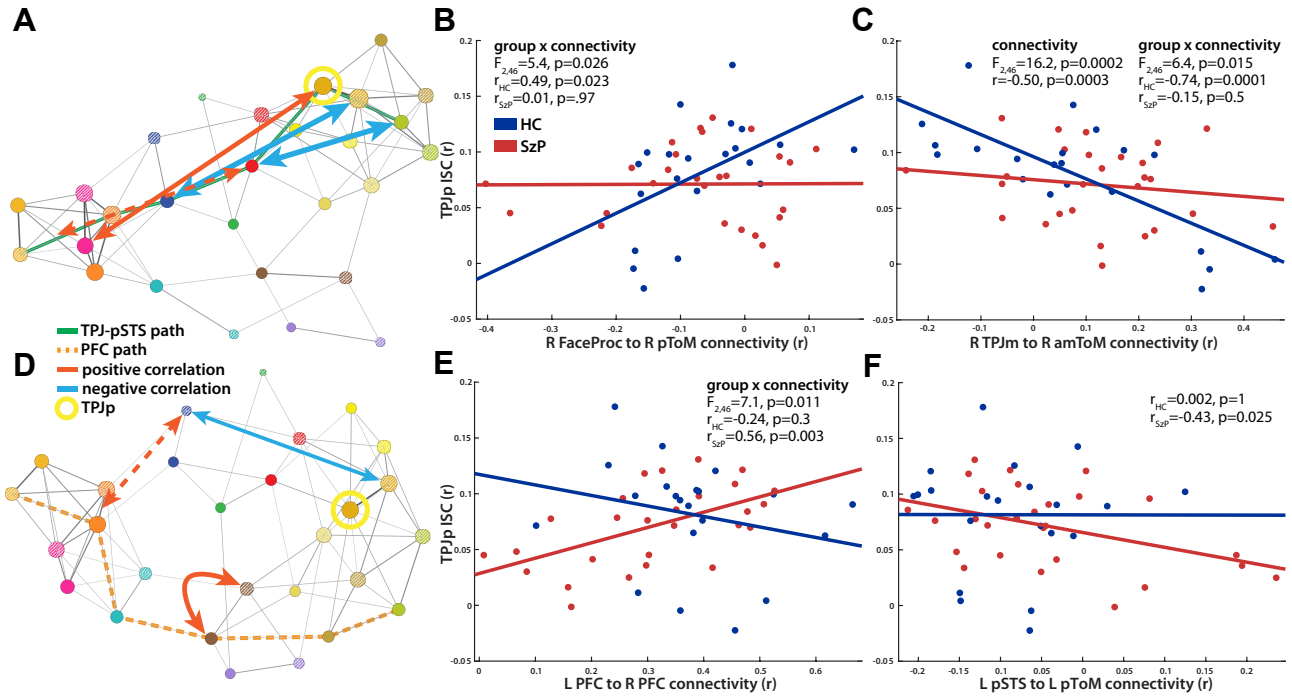

Figure 5. Relationship between connectivity strength between temporoparietal junction (TPJ)–posterior superior temporal sulcus (pSTS) and prefrontal cortex (PFC) path components and posterior TPJ (TPJp) activation as measured by intersubject correlation (ISC). **(A)** Positive (dark orange) and negative (light blue) connections significantly associated with TPJp ISC in healthy control subjects (HC). Dotted orange line shows the visual/face processing (FaceProc) to right (R) middle TPJ connection negatively correlated with the R middle TPJ to R anteromedial theory-of-mind (amToM) connection in HCs. **(B)** Relationship of the positive connection (R FaceProc to R posterior ToM [pToM]) with TPJp ISC in both groups. **(C)** Relationship of negative connection (R TPJm to R amToM) with TPJp ISC in both groups. The relationship for the other negative connection (left [L] pToM to R pSTS) is similar (connectivity: $F_{2,46}$ = 8.3, p = .006; r_{HC} = −0.58, p_{HC} = .006; r_{SzP} = −0.29, p_{SzP} = .2). **(D)** Positive (dark orange) and negative (light blue) connections significantly associated with TPJp ISC in participants with schizophrenia (SzPs). Dotted dark orange line shows the late visual to L pSTS connection negatively correlated with the L pSTS to L pToM connection in HCs. **(E)** Relationship of the positive connection (L PFC to R PFC) with TPJp ISC in both groups. **(F)** Relationship of negative connection (L pSTS to L pToM) with TPJp ISC in both groups.

areas, and social cognition as measured by TASIT and other tests. Another aspect of the TPJ-pSTS that merits further investigation is the extent to which individual variation in areal boundaries affects the relationships discussed here. Nonetheless, the results shown here and in our related studies provide a framework of how areas within the TPJ-pSTS and across the cortex dynamically update models of other people's mental states in social situations with incoming sensory information to guide future behaviors. With this framework, we will be better able to guide both the creation of diagnostic biomarkers of social dysfunction and the development of treatment targets aimed at alleviating the suffering resulting from functional anomalies affecting the social perception systems.

ACKNOWLEDGMENTS AND DISCLOSURES

We thank the funding agencies who supported this work: National Institute of Mental Health (Grant Nos. K23MH108711, T32MH018870, R01MH123639, and R01MH121790 [to GHP]; Grant No. R01MH049334 [to DCJ]; and Intramural Research Program Grant No. ZIA MH002898 [to DAL and RAB]), Brain & Behavior Research Foundation (to GHP), American Psychiatric Foundation (to GHP), Sidney R. Baer, Jr. Foundation (to GHP), Leon Levy Foundation (to GHP), the Dana Foundation (to GHP), and the Herb and Isabel Stusser Foundation (to DCJ).

We would also like to thank Nicole MacIlvane for her comments on the manuscript.

Data will be made available after reasonable request to corresponding author.

GHP receives income and equity from Pfizer, Inc. through family. DCJ has equity interest in Glytech, AASI, and NeuroRx; serves on the board of Promentis; and has received consulting payments/honoraria from Takeda, Pfizer, FORUM, Glytech, Autifony, and Lundbeck within the past 2 years. All other authors report no biomedical financial interests or potential conflicts of interest.

ARTICLE INFORMATION

From the Department of Psychiatry (GHP, DCG, ECJ, DRR-B, JPS-P, LPB, JKL, JG, AM, KNO, DCJ), Columbia University, New York; Experimental Therapeutics (GHP, JPS-P, LPB, JKL, JG, DCJ), New York State Psychiatric Institute, New York; and Schizophrenia Research Division (AM, DCJ), Nathan Kline Institute for Psychiatric Research, Orangeburg, New York; University of California, Los Angeles (SCA), Los Angeles, California; University of Michigan Medical School (CCK), Ann Arbor, Michigan; and the Section on Cognitive Neurophysiology and Imaging (RAB, DAL), the National Institute of Mental Health, Bethesda, Maryland.

Address correspondence to Gaurav H. Patel, M.D., Ph.D., at ghp2114@cumc.columbia.edu.

Received Sep 15, 2021; revised Mar 2, 2022; accepted Mar 6, 2022.

Supplementary material cited in this article is available online at https://doi.org/10.1016/j.bpsgos.2022.03.008.

REFERENCES

1. Kennedy DP, Adolphs R (2012): The social brain in psychiatric and neurological disorders. Trends Cogn Sci 16:559–572.
2. Patel GH, Sestieri C, Corbetta M (2019): The evolution of the temporoparietal junction and posterior superior temporal sulcus. Cortex 118:38–50.
3. Koster-Hale J, Saxe R (2013): Theory of mind: A neural prediction problem. Neuron 79:836–848.
4. Patel GH, Arkin SC, Ruiz-Betancourt DR, Plaza FI, Mirza SA, Vieira DJ, *et al.* (2021): Failure to engage the temporoparietal junction/posterior superior temporal sulcus predicts impaired naturalistic social cognition in schizophrenia. Brain 144:1898–1910.
5. Green MF, Horan WP, Lee J (2015): Social cognition in schizophrenia. Nat Rev Neurosci 16:620–631.
6. Green MF, Horan WP, Lee J (2019): Nonsocial and social cognition in schizophrenia: Current evidence and future directions. World Psychiatry 18:146–161.
7. Laumann TO, Snyder AZ (2021): Brain activity is not only for thinking. Curr Opin Behav Sci 40:130–136.
8. Bullmore E, Sporns O (2012): The economy of brain network organization. Nat Rev Neurosci 13:336–349.
9. Pitcher D, Ungerleider LG (2021): Evidence for a third visual pathway specialized for social perception. Trends Cogn Sci 25:100–110.
10. McDonald S, Flanagan S, Rollins J, Kinch J (2003): TASIT: A new clinical tool for assessing social perception after traumatic brain injury. J Head Trauma Rehabil 18:219–238.
11. Patel GH, Arkin SC, Ruiz-Betancourt DR, DeBaun HM, Strauss NE, Bartel LP, *et al.* (2021): What you see is what you get: Visual scanning failures of naturalistic social scenes in schizophrenia. Psychol Med 51:2923–2932.
12. Arkin SC, Ruiz-Betancourt D, Jamerson EC, Smith RT, Strauss NE, Klim CC, *et al.* (2020): Deficits and compensation: Attentional control cortical networks in schizophrenia. Neuroimage Clin 27:102348.
13. Hasson U, Nir Y, Levy I, Fuhrmann G, Malach R (2004): Intersubject synchronization of cortical activity during natural vision. Science 303:1634–1640.
14. Glasser MF, Sotiropoulos SN, Wilson JA, Coalson TS, Fischl B, Andersson JL, *et al.* (2013): The minimal preprocessing pipelines for the Human Connectome Project. Neuroimage 80:105–124.
15. Power JD, Mitra A, Laumann TO, Snyder AZ, Schlaggar BL, Petersen SE (2014): Methods to detect, characterize, and remove motion artifact in resting state fMRI. Neuroimage 84:320–341.
16. Gratton C, Dworetsky A, Coalson RS, Adeyemo B, Laumann TO, Wig GS, *et al.* (2020): Removal of high frequency contamination from motion estimates in single-band fMRI saves data without biasing functional connectivity. Neuroimage 217:116866.
17. Martínez A, Tobe RH, Gaspar PA, Malinsky D, Dias EC, Sehatpour P, *et al.* (2022): Disease-specific contribution of pulvinar dysfunction to impaired emotion recognition in schizophrenia. Front Behav Neurosci 15:787383.
18. Patel GH, Yang D, Jamerson EC, Snyder LH, Corbetta M, Ferrera VP (2015): Functional evolution of new and expanded attention networks in humans [published correction appears in Proc Natl Acad Sci U S A 2015; 112:E5377]. Proc Natl Acad Sci U S A 112:9454–9459.
19. Patel GH, Shulman GL, Baker JT, Akbudak E, Snyder AZ, Snyder LH, Corbetta M (2010): Topographic organization of macaque area LIP. Proc Natl Acad Sci U S A 107:4728–4733.
20. Jacoby N, Bruneau E, Koster-Hale J, Saxe R (2016): Localizing pain matrix and theory of mind networks with both verbal and non-verbal stimuli. Neuroimage 126:39–48.
21. Glasser MF, Coalson TS, Robinson EC, Hacker CD, Harwell J, Yacoub E, *et al.* (2016): A multi-modal parcellation of human cerebral cortex. Nature 536:171–178.
22. Woodward ND, Rogers B, Heckers S (2011): Functional resting-state networks are differentially affected in schizophrenia. Schizophr Res 130:86–93.
23. Baker JT, Holmes AJ, Masters GA, Yeo BTT, Krienen F, Buckner RL, Ongür D (2014): Disruption of cortical association networks in schizophrenia and psychotic bipolar disorder. JAMA Psychiatry 71:109–118.
24. Whitfield-Gabrieli S, Thermenos HW, Milanovic S, Tsuang MT, Faraone SV, McCarley RW, *et al.* (2009): Hyperactivity and hyperconnectivity of the default network in schizophrenia and in first-degree relatives of persons with schizophrenia [published correction appears in Proc Natl Acad Sci U S A 2009; 106:4572]. Proc Natl Acad Sci U S A 106:1279–1284.
25. Baker JT, Dillon DG, Patrick LM, Roffman JL, Brady RO Jr, Pizzagalli DA, *et al.* (2019): Functional connectomics of affective and psychotic pathology. Proc Natl Acad Sci U S A 116:9050–9059.
26. Croxson PL, Forkel SJ, Cerliani L, de Schotten MT (2018): Structural variability across the primate brain: A cross-species comparison. Cereb Cortex 28:3829–3841.
27. Reardon PK, Seidlitz J, Vandekar S, Liu S, Patel R, Park MTM, *et al.* (2018): Normative brain size variation and brain shape diversity in humans. Science 360:1222–1227.
28. Sotiras A, Toledo JB, Gur RE, Gur RC, Satterthwaite TD, Davatzikos C (2017): Patterns of coordinated cortical remodeling during adolescence and their associations with functional specialization and evolutionary expansion. Proc Natl Acad Sci U S A 114:3527–3532.
29. Butler PD, Abeles IY, Weiskopf NG, Tambini A, Jalbrzikowski M, Legatt ME, *et al.* (2009): Sensory contributions to impaired emotion processing in schizophrenia. Schizophr Bull 35:1095–1107.
30. Javitt DC (2009): When doors of perception close: Bottom-up models of disrupted cognition in schizophrenia. Annu Rev Clin Psychol 5: 249–275.
31. Martínez A, Tobe R, Dias EC, Ardekani BA, Veenstra-VanderWeele J, Patel G, *et al.* (2019): Differential patterns of visual sensory alteration underlying face emotion recognition impairment and motion perception deficits in schizophrenia and autism spectrum disorder. Biol Psychiatry 86:557–567.
32. Martínez A, Hillyard SA, Dias EC, Hagler DJ Jr, Butler PD, Guilfoyle DN, *et al.* (2008): Magnocellular pathway impairment in schizophrenia: Evidence from functional magnetic resonance imaging [published correction appears in J Neurosci 2008; 28:9319. J Neurosci 28:7492–7500.
33. McCleery A, Wynn JK, Lee J, Reavis EA, Ventura J, Subotnik KL, *et al.* (2020): Early visual processing is associated with social cognitive performance in recent-onset schizophrenia. Front Psychiatry 11:823.
34. Pinkham AE, Penn DL, Green MF, Buck B, Healey K, Harvey PD (2014): The social cognition psychometric evaluation study: Results of the expert survey and RAND panel. Schizophr Bull 40:813–823.
35. Gur RE, McGrath C, Chan RM, Schroeder L, Turner T, Turetsky BI, *et al.* (2002): An fMRI study of facial emotion processing in patients with schizophrenia. Am J Psychiatry 159:1992–1999.
36. Kim J, Park S, Blake R (2011): Perception of biological motion in schizophrenia and healthy individuals: A behavioral and FMRI study. PLoS One 6:e19971.
37. Buckner RL, Krienen FM, Yeo BTT (2013): Opportunities and limitations of intrinsic functional connectivity MRI. Nat Neurosci 16:832–837.
38. Newbold DJ, Laumann TO, Hoyt CR, Hampton JM, Montez DF, Raut RV, *et al.* (2020): Plasticity and spontaneous activity pulses in disused human brain circuits. Neuron 107:580–589.e6.
39. Sliwa J, Freiwald WA (2017): A dedicated network for social interaction processing in the primate brain. Science 356:745–749.
40. Betzel RF, Gu S, Medaglia JD, Pasqualetti F, Bassett DS (2016): Optimally controlling the human connectome: The role of network topology. Sci Rep 6:30770.
41. Rubinov M, Sporns O (2010): Complex network measures of brain connectivity: Uses and interpretations. Neuroimage 52:1059–1069.